Abbasirad and Ghotbi-Ravandi
BMC Plant Biology (2025) 25:187
https://doi.org/10.1186/s12870-025-06213-6

BMC Plant Biology

RESEARCH

Open Access

Toxicity of copper oxide nanoparticles in barley: induction of oxidative stress, hormonal imbalance, and systemic resistances

Sarasadat Abbasirad[1] and Ali Akbar Ghotbi-Ravandi[1*]

Abstract

Background Over the years, nanoparticles have emerged as a promising approach for improving crop growth, yield, and overall agricultural sustainability. However, there has been growing concern about the potential adverse effects of nanoparticles in the agricultural sector and the environment. The present study aimed to investigate the detrimental effects of high (1000 mg L^{-1}) concentrations of copper oxide nanoparticles (CuO NPs) on barley seedlings. The equivalent concentrations of CuO bulk and the ionic form of copper were also used in the experiments for comparative analysis. CuO NPs were characterized by Field Emission-Scanning Electron Microscopy, Dynamic Light Scattering, Zeta Potential analysis, and X-ray Diffraction prior to the application. Barley seedlings were subjected to the foliar application of CuO NP, CuO bulk, ionic Cu, and control group. The presence of CuO NPs in barley leaves was confirmed 72 hours after treatment by energy-dispersive X-ray analysis.

Results The results showed a CuO NPs treatment led to an impairment of nutrient balance in barley leaves. An increase in hydrogen peroxide content followed by the higher specific activity of catalase and ascorbate peroxidase was also observed in response to CuO NPs, CuO bulk, and Cu^{2+} ions. The profile of phytohormones including auxins (IAA and IBA), Gibberellins (GA_1, GA_4, and GA_9), abscisic acid (ABA), ethylene (ET), and jasmonic acid (JA) significantly affected by CuO NPs, CuO bulk, and Cu^{2+} ions. The transcripts of the *PR1* gene involved in systemic acquired resistance (SAR) and *LOX*-1 and *PAL* involved in induced systemic resistance (ISR) were significantly upregulated in response to CuO NPs treatment.

Conclusion Our findings suggest that the systemic resistances in barley seedlings were induced by higher accumulation of ABA, ET, and JA under CuO NPs treatment. The activation of systemic resistances indicated the involvement of both SAR and SAR pathways in the response to CuO NPs in barley.

Keywords Abiotic stress, Antioxidant enzymes, *Hordeum vulgare*, Phytohormones, Heavy metals, Engineered nanoparticles

Background

In recent decades, the fields of nanotechnology developed rapidly, resulting in the emergence of a plethora of nanomaterials with diverse applications. Nanoparticles (NPs) is a group of very small atoms or molecules, characterized by at least one dimension measuring less than 100 nm. They can be natural or man-made and have a significant surface area to volume ratio [1–4]. Compared to bulk form, nanomaterials possess distinct physical and

*Correspondence:
Ali Akbar Ghotbi-Ravandi
a_ghotbi@sbu.ac.ir
[1] Department of Plant Sciences and Biotechnology, Faculty of Life Sciences and Biotechnology, Shahid Beheshti University, Tehran, Iran

chemical characteristics, which include a higher surface area-to-volume ratio, unique size and shape, crystal structure, thermal stability, and charge [5, 6].

The NPs incorporation into agriculture has gained significant attention due to their potential benefits in enhancing plant growth, increasing yield, reducing chemical usage, and overall agricultural sustainability [7]. Despite the benefits of NPs, there has been growing concern about the potentially adverse effects of NPs on living entities [8, 9]. Cota-Ruiz et al. suggested that plants are capable of accumulating nanoparticles [10]. In particular, evidence indicates that the accumulation of NPs within plant tissues could potentially lead to adverse outcomes that may negatively impact agricultural yield, ecological balance, and human well-being [11, 12]. As NPs can be easily transported across the soil-water-plant interface, they can readily infiltrate plants and interact with biological processes, causing unpredictable toxic effects. For instance, it has been demonstrated that the accumulation of silver nanoparticles (Ag NPs), in plant tissues, imposes severe phytotoxicity at various levels ranging from morphological to molecular aspects [13].

Copper ions (Cu^{2+}), a common form of copper in soils, pose significant toxicity risks to plants due to their high mobility and adsorption capacity. Cu^{2+} ions are readily absorbed by plants, often leading to the disruption of physiological processes such as photosynthesis, enzymatic activity, nutrient balance and hormonal homeostasis [14, 15]. Excessive Cu^{2+} can generate reactive oxygen species (ROS), causing oxidative stress and damage to cellular components such as lipids, proteins, and DNA. Studies have demonstrated that Cu^{2+} toxicity can inhibit plant growth and development, reduce chlorophyll synthesis, and impair shoot and root elongation [16].

Among nanoparticles, copper oxide nanoparticles (CuO NPs) have emerged as a promising candidate for agricultural applications. CuO NPs possess unique physicochemical characteristics that render them appropriate for diverse agricultural applications such as plant protection, nutrient delivery, and soil remediation [5, 17]. Despite the potential benefits of CuO NPs in agriculture, their overuse can have deleterious effects on plants, due to their water solubility and tendency to accumulate in soil [18]. CuO NPs can accumulate in plant tissues, leading to potential phytotoxicity [19]. In addition, CuO NPs can also cause environmental pollution if they are not properly disposed of. Therefore, it is imperative to carefully evaluate the potential hazards associated with the application of CuO NPs in plant production.

Several studies have revealed exposure to varying levels of CuO NPs or Cu^{2+} ions result in the higher generation of reactive oxygen species (ROS) in different plant species. For instance, Shah et al. demonstrated that different concentrations of CuO NPs suppressed the growth rate and induced oxidative damage *Cucumis melo* seedlings [20]. Wang et al. reported that CuO NPs application led to inhibition of seedling growth, and pollen germination of different *Arabidopsis thaliana* ecotypes [21]. Moreover, other studies have also reported similar findings, indicating adverse impacts of CuO NPs on the growth, development, and physiological and molecular processes of plants [19, 22], indicating the unfavorable impact of CuO NPs on the proliferation, maturation, and biochemical and genetic mechanisms of plants.

Numerous studies have documented a link between NPs and phytohormones. Phytohormones not only play a regulatory role in plant growth and development, but also act as a pivotal element in the coordination of plants' tolerance mechanisms in response to external factors [23]. The exposure of cotton to CuO NPs resulted in a remarkable elevation in Abscisic acid (ABA) content. Moreover, the concentration of ABA exhibited a direct correlation with the dosage of the treatment. [24]. Furthermore, Gui et al. reported a rise in the concentrations of various phytohormones within the root systems of both transgenic and non-transgenic rice, upon exposure to γFe2O3NPs [25]. Exposure to nanoparticles could also lead to alteration of genes transcription concerned in biosynthetic or signaling pathways of some phytohormones, such as auxin repressor, ABA biosynthetic genes, and ethylene (ET) signal transduction components [26, 27].

Apart from regulating responses to abiotic factors, stress-related phytohormones are able to trigger systemic immune responses in plants affecting both pathogenic and beneficial microbe interactions. There are two main systemic defense mechanisms in plants that play a pivotal role during biotic interactions, namely SAR (systemic acquired resistance) and ISR (induced systemic resistance). These responses to biotic stresses are elicited through the action of phytohormones including ET, ABA, jasmonic acid (JA), and salicylic acid (SA) [28, 29].

Certain genes are associated with different defense pathways, such as PR proteins (pathogenesis-related proteins) typically expressed in conjunction with the SAR pathway, and the lipoxygenase (*LOX-1*) and phenylalanine ammonia-lyase (*PAL*) genes have been linked to the ISR pathway [28, 30]. Numerous reports have reported the enhanced expression of PR proteins under both biotic and abiotic stresses. PR proteins are instrumental in enhancing defense mechanisms in plants and serve as indicators for defense signaling pathways that confer enduring protection against stressors [31, 32]. Furthermore, Abdelkhalek and Al-Askar. discovered that spraying tomato plants with zinc oxide nanoparticles (ZnO NPs) either before or after being infected with the TMV (tobacco mosaic virus) increased the expression

of certain systemic immune genes including *PAL*, *PR-1*, *CHS*, and *POD* [33].

Barley holds significant importance as a cereal crop, cultivated extensively across the globe due to its economic value. Additionally, it serves as a valuable model for studying the plants response to environmental stresses and external factors. However, there is limited understanding of the impact of NPs on cereal crops like barley, particularly that of CuO NPs, on the signaling pathways of ISR and SAR through changes in phytohormones content and the expression of defense gene (*PR-1*, *PAL*, and *LOX-1*). In this context, understanding the effects of CuO NPs can provide insights into the detrimental impacts on various physiological and biochemical processes, plant health, and risk assessment.

Given the multifaceted functions of phytohormones in responding to external abiotic stresses and their role in triggering the systemic resistances, this study was designed with two main objectives. Firstly, we aimed to investigate the changes in the antioxidant activity and phytohormones level and possible activation of ISR and SAR pathways in barley in response to CuO NPs. Secondly, we aimed to compared and contrast these effects to impacts induced by bulk CuO and ionic form of Cu.

Methods

Characterization of CuO NPs

CuO NPs (size < 100 nm) and CuO bulk (100–10,000 nm) were purchased from Iranian Nanomaterials Pioneers Company. NPs were characterized by Field Emission-Scanning Electron Microscopy (FE-SEM, TESCAN MIRA, USA) (Supplementary Fig. 1), Dynamic Light Scattering (DLS) (Supplementary Fig. 2), Zeta potential analysis (DLS/ZETA Potential, Nano-flex2 Model, Germany) (Supplementary Table 1), and X-ray Diffraction (XRD, Philips PW1730, Netherlands) (Supplementary Fig. 3). Seventy-two hours after the foliar application of CuO NP solution (Refer to section 2.3) on barley leaves, Energy-dispersive X-ray (EDX) analysis was performed using a Scanning Electron Microscopy (FEI ESEM QUANTA 200, USA) configured with an EDAX EDS system (EDAX EDS Silicon Drift 2017 detector, USA) to confirm the existence of CuO NPs in barley leaves (Supplementary Figs. 4 and 5, Supplementary Tables 2 and 3).

Plant materials and growing condition

Seeds of barley (*Hordeum vulgare* L., Zehak cultivar) were obtained from the Seed and Plant Improvement Institute (SPII). The seed sterilization process involved brief immersion in 70% ethanol for two minutes, followed by a five-minute soak in 6% sodium hypochlorite solution. Afterward, the seeds were thoroughly rinsed with distilled water. Sterilized seeds were planted in 90 mm plastic pots, with a growing medium consisting of a mixture of two-thirds peat moss and one-third perlite. Pots were maintained under controlled environmental conditions, with a day/night temperature range of 25 ± 2°C (16 hours of light) to 20 ± 2°C (8 hours of darkness). The humidity was maintained at 65–70%, and the plants received a light intensity of 340 μmol $m^{-2}s^{-1}$ for three weeks. All plants received daily irrigation with deionized water and weekly half-strength Haugland solution throughout the cultivation period.

Preparation and application of CuO NPs, CuO bulk, and ionic Cu suspension/solution

In this study, micro and nano-sized copper oxide were used as counterparts to compare the effect of copper at different sizes, whereas the ionic form of Cu was used to distinguish the impacts of ions and particles. Suspensions of CuO NPs and CuO bulk were prepared at 1000 mg. L^{-1} in 250 mL volumetric flasks, using Millipore water. The ionic copper solution was prepared by dissolving 2 g of copper sulfate ($CuSO_4.5H_2O$) (Cu content equal to the Cu content of in nano and bulk suspension) in 250 ml of deionized water. In order to prevent aggregation, suspensions, and solutions underwent a 30-min sonication process using an ultrasonic water bath at a temperature range of 20–25°C and a power output of 180 watts. (Model Elma S30/H - HU193, Germany). Twenty-one days after sowing, pots were randomly divided into 4 groups (Control, CuO NP treatment, CuO bulk treatment, and ionic Cu treatment). The respective solutions were applied by spraying on the leaf surface of the plants, while the control group received deionized water. Samples were carefully taken 72 hours after foliar treatment from identical phyllotaxis positions. The external Cu was removed from the leaves by rinsing before drying or preservation at − 80°C.

Measurement of Cu and other nutrients content

Dried barley leaves were subjected to digestion utilizing 5 mL of HNO_3 (67–70%) and heated for a duration of 45 minutes at 115°C on a DigiPREP MS digestion block (SCP Science, NY) and were subsequently diluted to a 50 mL volume using Millipore water and were analyzed utilizing inductively coupled plasma optical emission spectroscopy (ICP-OES, Perkin-Elmer Optima 8300 DV) [34].

Determination of hydrogen peroxide (H_2O_2) content

Fresh leaves (0.5 g) were first blended in a solution containing 0.01% trichloroacetic acid (TCA) and then subjected to centrifugation at 12,000 g for 15 minutes at a temperature of 4 degrees Celsius. After centrifugation, the resulting supernatant was combined with 500 μL of a phosphate buffer (100 mM) and 2 ml of a 1 M potassium

iodide solution. This mixture was then left in the dark for one hour. Subsequently, the absorbance of the resulting solution was measured at a wavelength of 390 nm using a spectrophotometer (Shimadzu UV-1601PC, Japan). The concentration of hydrogen peroxide (H_2O_2) in the samples was determined by comparing the absorbance to a standard curve generated by measuring the absorbance of H_2O_2 standard solutions prepared in 1% TCA. The results were expressed in µmol per gram (µmol. g^{-1}) [35].

Determination of antioxidant enzymes activity

Leaf samples (0.25 g) were finely ground in an ice-cold mortar, with the addition of a 100 mM phosphate buffer (pH 7) that also contained 1% PVP (Polyvinylpyrrolidone) and 1mM EDTA (Ethylenediaminetetraacetic acid). Following homogenization, the mixtures were then subjected to centrifugation at 10,000 g for 15 minutes at 4°C. The resulting supernatants were divided into smaller portions (aliquots) and stored at −20°C for subsequent measurements of antioxidant enzyme activity. Furthermore, the protein content in these samples was determined based on Bradford [36].

Determination of catalase (CAT) specific activity was conducted based on the method described by Aebi [37]. To initiate the enzymatic reaction, 100 µl of enzyme extract was added to a mixture consisting of 1 ml of potassium phosphate buffer (50 mM, pH 7.0) and 100 µl of H_2O_2 (100 mM). Over a period of 3 minutes, the changes in absorbance resulting from the decomposition of H_2O_2 were monitored at a wavelength of 240 nm. The specific activity of catalase was quantified and expressed as U. mg $protein^{-1}$.

The specific activity of ascorbate peroxidase (APX) was conducted following the protocol outlined by Nakano and Asada [38]. To initiate the reaction, a 1 ml mixture was prepared, comprising 50 mM potassium phosphate (pH 7), 0.2 mM EDTA, 0.5 mM ascorbic acid, and 50 µl of enzyme extract. The addition of H_2O_2 (0.25 mM) to the mixture triggered the reaction, and the absorbance was recorded at a wavelength of 290 nm over a 3-minute period. The activity of APX was quantified and expressed as U. mg $protein^{-1}$.

The specific activity of superoxide dismutase (SOD) was assessed by determining the inhibition of photochemical reduction of NBT (nitroblue tetrazolium) following the method outlined by Giannopolitis and Ries [39]. The reaction mixture comprised 195 mL of 0.1 M potassium phosphate buffer (pH 7.5), 150 mM methionine, 1.2 mM Na_2EDTA, 24 µM riboflavin, 840 µM NBT, and 50 µL of plant extract. The reaction was initiated by exposing this mixture to light. As a reference, an identical solution without exposure to light was used as a blank. Furthermore, a control was prepared by subjecting an irradiated reaction mixture to light without including enzyme extract. To measure SOD activity, the absorbance of the samples was recorded at 560 nm using a spectrophotometer. One unit (U) of SOD activity was defined as the quantity of enzyme necessary to cause a 50% reduction in the NBT reduction reaction within one minute. The data were expressed as units per milligram of protein (U. mg^{-1} protein).

Determination of phytohormones content

Phytohormones were extracted by the method described by Singh et al. [40]. Barley leaves (1 gr) were finely blended in a solution of 80% methanol, and 100 mg. l^{-1} BTH (butylated hydroxytoluene). After homogenization, these mixtures were left in the dark at a temperature of 4°C overnight. Additionally, stable isotope-labeled hormones were introduced as internal standards for analysis. The mixture then was subjected to a freezing and thawing process, and centrifugated at 9000×g at 4°C for 30 minutes. the resulting solution was then vacuum-evaporated using a Buchi Rotavapor Re Type apparatus. Afterward, the solution was redissolved methanol (1 ml, HPLC grade) and filtered prior to analysis. The phytohormones content was determined by an HPLC system (Agilent 1260, Agilent, USA) equipped with binary 1260 infinity LC G1312B reciprocating pumps, a variable UV-VIS detector system (G1314F VWD UV detector, Agilent), an integrator, and Agilent Lab Advisor software. Reverse-phase chromatography was performed using a C-18 reverse-phase HPLC column according to Liu et al [41]. The running conditions consisted of a mobile phase comprising methanol: 0.4% acetic acid (80:20, vol/vol), flow rate set at 1.0 ml/min, injection volume of 5 µm, and detection at 290 nm. Both internal and external standards such as ABA, SA, JA, Indole-3-acetic acid (IAA), Indole-3-butyric acid (IBA), trans-zeatin (t-ZR), dihydrozeatin (DHZ), and gibberellins (GAs) were employed. To qualitatively characterize the compounds, co-injection and retention time (Rt) were compared. Moreover, the peak areas of the reference compounds were compared with those of the samples analyzed under identical elution conditions to determine the concentrations of the compounds.

The leaf samples were placed in vials containing filter paper soaked in 1 ml of deionized water and sealed with rubber serum caps. The samples were then incubated in darkness at a temperature of 27°C on a rotating shaker (100 rev. mm) for six hours. After the incubation period, a gas sample of 1 ml was extracted from each flask's headspace, and subsequently, the content of ethylene was assessed using a Shimadzu GC-MS model QP2010 SE gas chromatograph that was fitted with a flame ionization

detector, an alumina column, a turbomolecular pump, and a rotary pump.

Gene expression analysis

The specific primers for lipoxygenase 1 (*LOX-1*), Pathogenesis-related protein1 (*PR-1*), and Phenylalanine ammonia-lyase 1 (*PAL-1*) were designed based on the sequences from the NCBI database by Vector NTI software (Supplementary Table 4). RNA extraction and quantification, cDNA synthesis, and quantitative real-time PCR were performed according to Ahangir et al. [42]. Actin served as an internal control for normalization. The relative expression genes and statistical significance were assessed by REST software [43].

Statistical analysis

The experiments were structured using a complete randomized design (CRD). The results represent the means of three independent replications, and standard error (SE) is indicated. After confirming the normal distribution of data, statistical assessment was carried out using analysis of variance (ANOVA) at a significance level of $P \leq 0.05$. Subsequently, Duncan's multiple range test was conducted to compare the means, and all analyses were performed using SPSS software (version 21).

Results

Nutritional status

The result of the application of CuO NPs, CuO bulk, and Cu^{2+} ions on nutrient content in barley leaves is presented in Table 1. Leaf copper (Cu) content significantly increased in response to all treatments. The Cu^{2+} ion treatment led to a significant 15.67-fold increase in Cu content in barley leaves. Furthermore, the CuO NPs and CuO bulk treatment significantly increased Cu content by 77% and 26%, respectively, as compared to the control. The application of CuO NPs, CuO bulk, and Cu^{2+} ions resulted in a significant ($P \leq 0.05$) reduction of leaf nitrogen (N) content by 19%, 8%, and 24%, respectively. The calcium (Ca) content declined by approximately 28% under both the CuO NPs and Cu^{2+} ions exposure. The CuO bulk treatment caused an 8% decrease in the leave Ca content, as compared to the control group. The leaf zinc (Zn) content decreased by 43%, 27%, and 52% in response to CuO NPs, CuO bulk, and Cu^{2+} ions treatments, respectively, as compared to the control group. Similarly, the application of CuO NPs, CuO bulk, and Cu^{2+} ions led to a significant ($P \leq 0.05$) reduction (36%, 43%, and 16% reduction, respectively) in the magnesium (Mg) content of barley leaves.

Hydrogen peroxide content (H_2O_2) and antioxidant enzymes activities

The barley seedlings exhibited a significant increase ($P \leq 0.05$) in their hydrogen peroxide content by 33% upon the application of CuO NPs. Furthermore, the application of CuO bulk, and Cu^{2+} ions caused a significant ($P \leq 0.05$) elevation of 20% and 43% in the H_2O_2 content, respectively, as compared to the control group (Fig. 1a).

The specific activity of the SOD enzyme in barley leaves remained unaffected by the application of CuO NPs and CuO bulk, whereas the addition of Cu^{2+} ions resulted in a significant increase (22%) in the SOD activity (Fig. 1b).

Application of CuO NPs, CuO bulk, and Cu^{2+} ions significantly increased ($P \leq 0.05$) the specific activity of APX and CAT in barley leaves. The highest activity of these two enzymes was observed in Cu^{2+} ions treatments (Fig. 1c, d). The specific activity of APX increased 1.82-fold, 1.48-fold, and 2.16-fold in response to CuO NPs, CuO bulk, and Cu^{2+} ions treatment, respectively (Fig. 1c). Similarly, the specific activity of CAT exhibited a 57%, 37%, and 89% increase in response to the application of CuO NPs, CuO bulk, and Cu^{2+} ions, respectively (Fig. 1d).

Phytohormone content

Significant alterations in the phytohormones content of barley seedlings were observed as a result of CuO NPs, CuO bulk, and Cu^{2+} ions treatments. The IAA content exhibited a significant decrease ($P \leq 0.05$) in all three CuO NPs, CuO bulk, and Cu^{2+} ion treatments, as compared to the control group. The highest decrease in IAA

Table 1 Effects of CuO NPs, CuO bulk, and Cu ion treatments on nutrient contents in the leaves of barley. Data are presented as mean ± standard Error (SE). Different letters indicate a significant difference ($p \leq 0.05$) according to Duncan's multiple range test

Treatment	Nutrient content (μg.g^{-1})				
	Cu	Ca	Zn	N	Mg
Control	6.86 ± 0.11 d	1.57 ± 0.00 a	334.43 ± 5.57 a	16.73 ± 0.20 a	1.06 ± 0.01 a
CuO NPs	12.19 ± 0.28 b	1.10 ± 0.01 c	187.30 ± 17.33 c	13.51 ± 0.38 c	0.67 ± 0.05 c
CuO bulk	8.67 ± 0.52 c	1.44 ± 0.01 b	240.94 ± 12.06 b	15.25 ± 0.09 b	0.88 ± 0.02 b
Cu ion	15.70 ± 0.13a	1.12 ± 0.00 c	159.59 ± 12.69 c	12.56 ± 0.46 c	0.60 ± 0.06d c

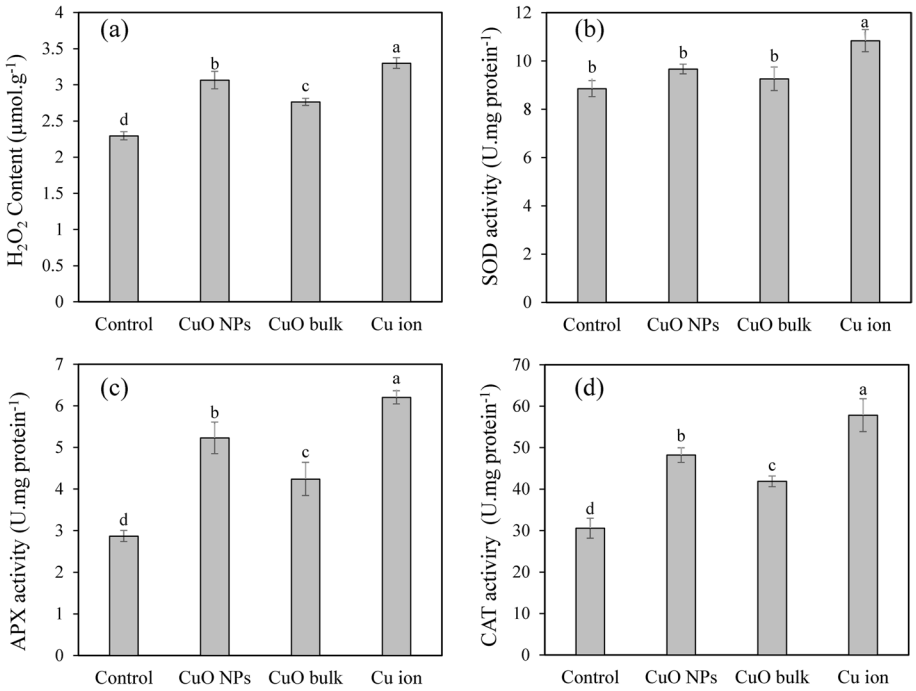

Fig. 1 Effects of CuO NPs, CuO bulk, and Cu ion treatments on H_2O_2 content (**a**), activity of superoxide dismutase (**b**), ascorbate peroxidase (**c**), and catalase (**d**) enzymes in barley leaves. Data are presented as mean ± standard error (SE). Different letters indicate a significant difference ($p \leq 0.05$) according to Duncan's multiple range test.

content was observed in Cu^{2+} ion (57%) and CuO NPs (52%) treatments (Fig. 2a). The IBA content significantly ($P \leq 0.05$) reduced by 76%, 71%, and 79% in CuO NPs, CuO bulk, and Cu^{2+} ion treatments, respectively, as compared to the control. However, no significant differences were observed between the different treatments (Fig. 2b).

Figure 3 depicts the effects of CuO NPs, CuO bulk, and Cu^{2+} ions treatments on the gibberellins content in barley leaves. The application of CuO NPs and Cu^{2+} led to a significant ($P \leq 0.05$) decrease in the GA_1, GA_4, and GA_9 content in barley leaves, as compared to the control group (Fig. 3). Nevertheless, the utilization of CuO bulk merely resulted in a significant decrease in the GA_9 component and did not exert a considerable impact on the concentrations of GA_1 and GA_4. Application of CuO NPs and Cu^{2+} ion treatments resulted in an approximate reduction of 62% and 69%, in GA_1, and 51% and 39%, in GA_4 content, respectively. An 83%, 78%, and 54% reduction in the GA_9 content was observed in CuO NPs, CuO bulk, and Cu^{2+} ions treatments, respectively.

The impacts of CuO NPs, CuO bulk, and Cu^{2+} ions treatments on the cytokinins content of barley leaves are presented in Fig. 4. The content of *trans*-zeatin (Fig. 4a) and dihydrozeatin (Fig. 4b) were not significantly ($P \leq 0.05$) affected by either of the treatments.

The content of stress-related phytohormones in barley leaves also affected the application of CuO NPs, CuO bulk, and Cu^{2+} ions (Fig. 5). The content of JA significantly ($P \leq 0.05$) increased in response to CuO NPs and Cu^{2+} ions treatments and exhibited a 1.73 and 2.03-fold increase compare to the control, respectively, whereas, CuO bulk application, did not affect the JA content (Fig. 5a).

CuO NPs, CuO bulk, and Cu^{2+} ions treatment led to a 46%, 20%, and 60% increase in ET content, respectively (Fig. 5b). Notably, the highest increase was observed in plants treated with Cu^{2+} ions.

The imposed CuO NPs, CuO bulk, and Cu^{2+} ions treatments led to a significant ($P \leq 0.05$) decrease in the SA content of barley leaves (Fig. 5c). The most significant decline in SA content was recorded in Cu^{2+} ions treatment by approximately 95%, as compared to the control group. Furthermore, the application of CuO NPs and CuO bulk also led to a significant decline of 73% and 44% in SA content, respectively.

All CuO NPs, CuO bulk and Cu^{2+} ions treatments resulted a significant ($P \leq 0.05$) rise in ABA levels, as compared to the control group. The use of CuO NPs, CuO bulk, and Cu^{2+} resulted in 43.0, 35.33, and 44.68-fold increases in ABA content of barley leaves, respectively (Fig. 5d).

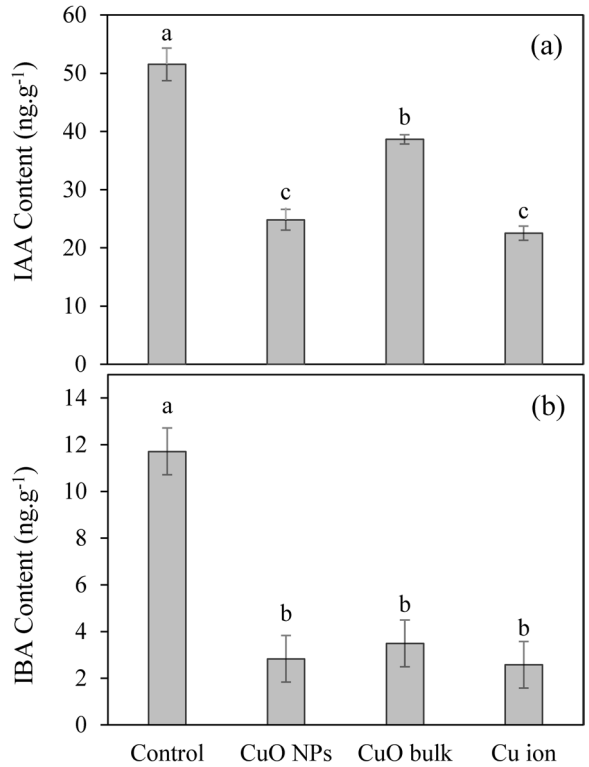

Fig. 2 Effects of CuO NPs, CuO bulk, and Cu ion treatments on the Indole 3- acetic acid (**a**) and Indole 3-butyric acid (**b**) content of barley leaves. Data are presented as mean ± standard error (SE). Different letters indicate a significant difference ($p \leq 0.05$) according to Duncan's multiple range test

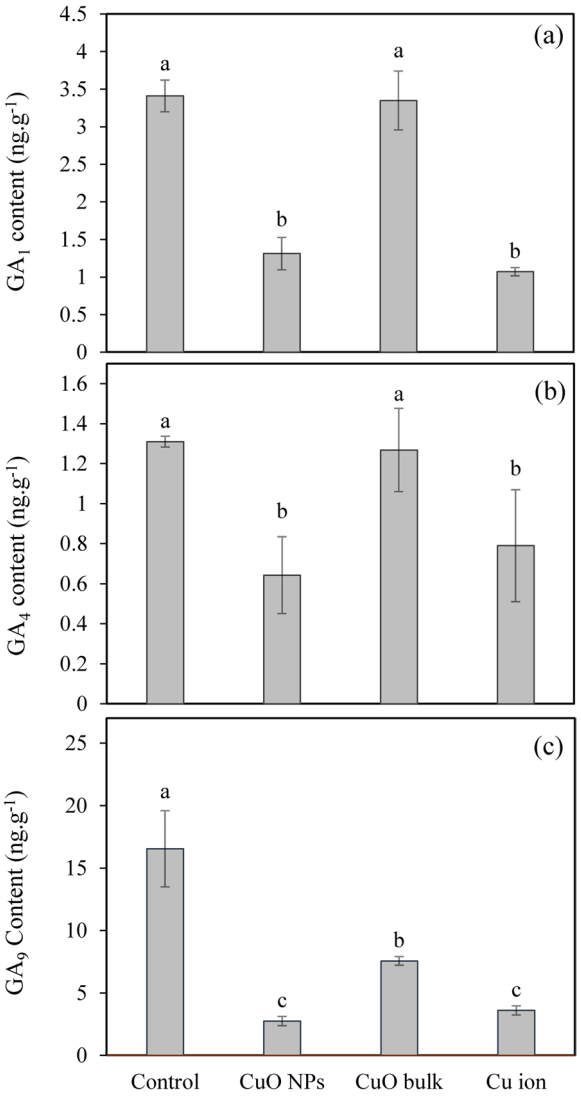

Fig. 3 Effects of CuO NPs, CuO bulk, and Cu ion treatments on the gibberellins content of barley leaves. Data are presented as mean ± standard error (SE). Different letters indicate a significant difference ($p \leq 0.05$) according to Duncan's multiple range test

Alteration in the gene expression patterns

Quantitative real-time PCR results revealed that exposure to CuO NPs, CuO bulk, and Cu^{2+} ions significantly affected *LOX-1*, *PAL*, and *PR-1* gene expression in barley (Fig. 6). A significant up-regulation of the *LOX-1* gene was observed in all treatments, particularly, CuO NPs and Cu^{2+} ions, resulting in of 7.63 and 7.35-fold increase, respectively. A significant increase in *PAL* gene transcripts was also observed in CuO NPs, CuO bulk, and Cu^{2+} ions treatments, with a 1.66, 1.55, and 5.75-fold increase, respectively, as compared to the control. Exposure to CuO NPs, CuO bulk, and Cu^{2+} ions led to the upregulation of *PR-1* gene with 4.56, and 1.47, and 64.35-fold compared to the control group.

Discussion

Several studies indicated that the growth rate and developmental process of crops can be adversely affected by the presence of metal and metal oxide nanoparticles [44]. This effect is most likely caused by the discharge of toxic metal ions from these nanoparticles [45, 46], which significantly reduces mineral absorption by plants [47–49]. In our study, foliar administration of CuO NPs resulted in a significant decline in the nutrient content of barley leaves. Consistent with our findings, the foliar application of Ag NPs (1000 $mg.L^{-1}$; size: 35 nm) led to the reduction in the mineral nutrient of tomato [50]. Similarly, Dimkpa et al. observed a reduction in the shoot concentration of Zn and Ca with the application of CuO NPs at sizes of 100, 250, and 500 $mg.kg^{-1}$ with a dimension of 50 nm [51]. Peralta-Videa et al. reported that the presence of even small amounts of CeO_2 and ZnO NPs in NP-amended soil can disrupt the absorption of crucial nutrients in soybean plants [52]. Furthermore, the alteration in nutrient content (Fe, Cu, Mg, Zn, and Na) in the

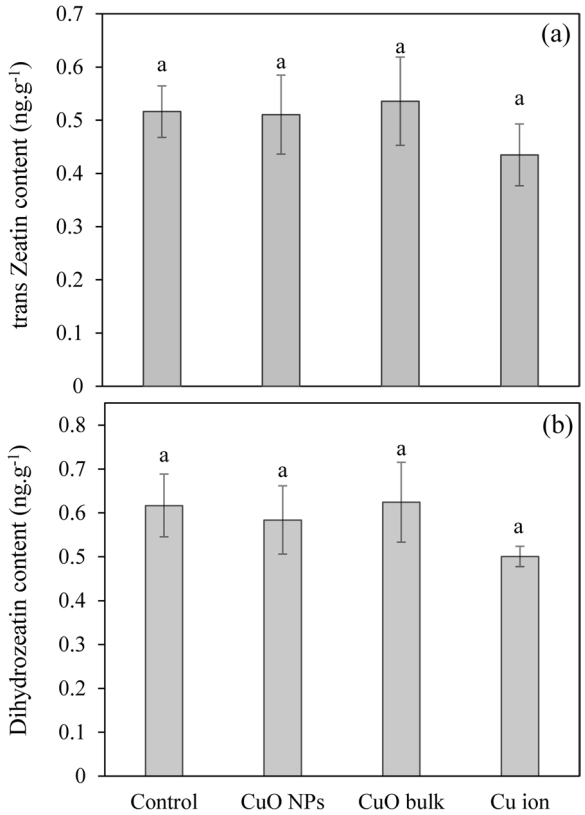

Fig. 4 Effects of CuO NPs, CuO bulk, and Cu ion treatments on the trans-zeatin (**a**), dihydrozeatin (**b**) content of barley leaves. Data are presented as mean ± standard error (SE). Different letters indicate a significant difference ($p \leq 0.05$) according to Duncan's multiple range test

transgenic cotton has been observed as a result of CeO_2 and SiO_2 NPs treatments [53–55].

In the current study, the contents of Cu in the barley leaves significantly increased due to CuO NPs treatment. The presence of nanoparticles in the leaves was also observed and verified through the utilization of SEM images (supplementary Figs. 4 and 5). Accumulation of Cu in alfalfa was also reported in response to the application of CuO NPs sized between 10–100 nm at concentrations of 5, 10, and 20 mg L^{-1} [56]. The notion that heavy metal elements restrict mineral absorption in plants has been widely accepted [48, 49]. In our study, the highest Cu content and the nutritional imbalance were observed in Cu^{2+} ion treatment followed by CuO NPs treatment and bulk CuO. Due to their small size, CuO NPs can be more readily taken up by plants compared to bulk CuO. CuO NPs may also release copper ions more rapidly than bulk CuO due to their higher surface area and dissolution rate. The higher nutrient imbalance CuO NP treatments compared to bulk CuO may be attributed to higher solubility and bioavailability, leading to increased competition with other essential elements. These findings suggest that while CuO NPs contribute to nutrient imbalances, the effects are not solely nanoparticle-specific but are also linked to the release of Cu^{2+} ions. The minor changes in nutrient contents of CuO bulk treatment can be attributed to the lower surface area and ionization rate. The observed reduction in nutrient content, such as Zn and Mg, can be attributed to the interference of Cu with the uptake of other essential elements. It has been reported that excessive Cu can inhibit the absorption pathways of other nutrients by interaction and competition with metal transporters. Furthermore, under Cu toxicity, alteration in the expression of genes involved in nutrient uptake can negatively affect nutrient homeostasis in plants[15, 16]

Copper-based NPs have been noted for their diverse range of shapes and oxidation states. CuO NPs are more hazardous than Cu NPs, due to their oxidizing characteristics. These nanoparticles can be further oxidized to either Cu^{+} (Cu_2O) or Cu^{2+} (CuO) [57], which give rise to the formation of ROS and oxidative stress. Higher generation of ROS, such as H_2O_2 can ultimately damage cell macromolecules [58]. Accumulation of CuO NPs in the plant affects the physiological processes that also induce ROS formation [59]. The present study highlights the significant elevation of H_2O_2 content in barley leaves upon exposure to different Cu treatments. The increased ROS generation in CuO NP-, bulk CuO, and Cu^{2+}-treated barley seedlings confirm that Cu-induced stress, rather than a nanoparticle-specific effect, plays a major role in triggering oxidative responses. However, the higher ROS accumulation observed in CuO NP treatments compared to bulk CuO suggests that nanoparticles, due to their increased surface area and dissolution rate, may exacerbate oxidative stress. The ability of CuO NPs to generate ROS has been documented in several studies, confirming their potential to induce stress responses in plants beyond what is observed with bulk materials. For example, Chung et al. reported that the generation of malondialdehyde (MDA) and H_2O_2 was also increased in *Brassica rapa ssp. rapa* treated with CuO NPs, ultimately leading to DNA damage as indicated by the DNA ladder test [60].

The harmful outcomes of ROS can be overcome by the activation of antioxidative enzymes responsible for the dismutation of superoxide (SOD) and H_2O_2-metabolism (APX and CAT). These enzymes play a crucial role in maintaining the equilibrium of ROS in plants [61, 62].

The process of converting H_2O_2 into water and oxygen is aided by enzymes APX and CAT in different cell organelles including chloroplasts, cytosol, mitochondria, and peroxisomes [63]. Our data revealed the heightened APX and CAT enzymatic activities in barley seedlings that were exposed to Cu^{2+} ions, CuO

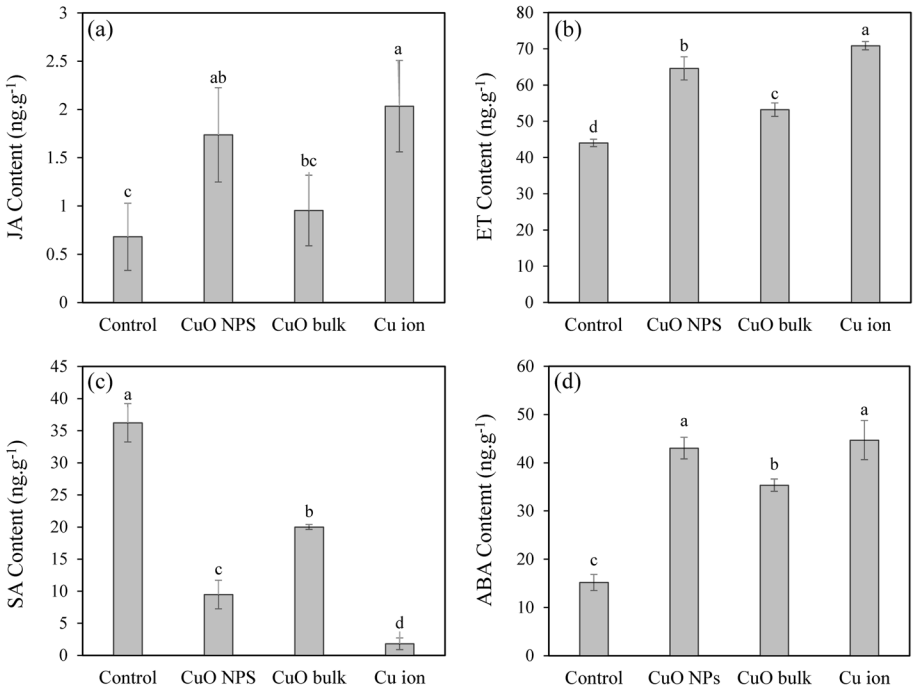

Fig. 5 Effects of CuO NPs, CuO bulk, and Cu ion treatments on the jasmonic acid (**a**), ethylene (**b**), salisylic acid (**c**), and abscisic acid (**d**) content of barley leaves. Data are presented as mean ± standard error (SE). Different letters indicate a significant difference ($p \leq 0.05$) according to Duncan's multiple range test

NPs, and CuO bulk treatments, respectively, which were proportionate to the H_2O_2 content of each treatment. Higher activity of APX and CAT have enabled the plants to effectively counteract the adverse effects of excessive H_2O_2 in tomato plants [64]. Yusefi-Tanha et al. indicated that the type and concentration of copper compounds, as well as their interactions differentially impacted MDA content and the activity of different antioxidant enzyme biomarkers, including SOD, CAT, POX, and APX in soybean (soil-grown *Glycine max)* [65]. Moreover, the impact of CuO NPs on the process of lipid peroxidation and the efficacy of antioxidant biomarkers in soybean leaves at 120 days after plantation was correlated with both the size of the particles and their concentration. In contrast, our findings are distinct from some other studies, which documented a decline in the activity of antioxidant enzymes such as CAT and APX under CuO NPs stress [56, 66]. Therefore, it is imperative to examine the varied effects of NPs on different enzymes, which are linked to factors such as dimension, surface area, concentration, and exposure time, as well as the age and species of the targeted plants [67]. The results of our study also demonstrate that the level of SOD activity was higher in response to Cu^{2+} ion treatment than CuO NPs and CuO bulk treatments, indicating of Cu^{2+} ions pose the most toxic effects within the plant cell.

Physiological and developmental processes in plants are regulated by chemical compounds commonly known as phytohormones. There are five primary plant growth hormones: Auxins (IAA and IBA), cytokinins (t-ZR and DHZ), GAs, ABA, and ET [22]. Other compounds like SA and JA, help plants defend against biological and environmental stressors [68, 69]. The presence of nanoparticles in plants may cause changes in phytohormone-related processes. This occurs due to the distribution and accumulation of NPs in different parts of the plant, which alters the synthesis, concentrations, and signaling pathways of specific phytohormones [70, 71].

In the present study, CuO NPs treatment imposed an adverse on the production of endogenous auxins (IAA and IBA) in barely compared to the control groups. This observation is in agreement with the suppression of IAA levels in *A.thaliana* under ZnO NPs [72]. In addition to hindering auxin biosynthesis, it has been reported that auxin signaling pathways can be negatively influenced by NPs [72]. Sun et al. suggested that Ag NPs, could be traversed plant cells via plasmodesmata and hinder the binding of auxin to its receptor [73]. Wang et al. reported that Cu NPs treatment led to a decrease in the expression of the auxin signaling F-box protein, involved in negative feedback regulation during auxin signaling process [21].

Our study showed that the application of Cu^{2+} ion, CuO bulk, and CuO NPs had no significant effect on

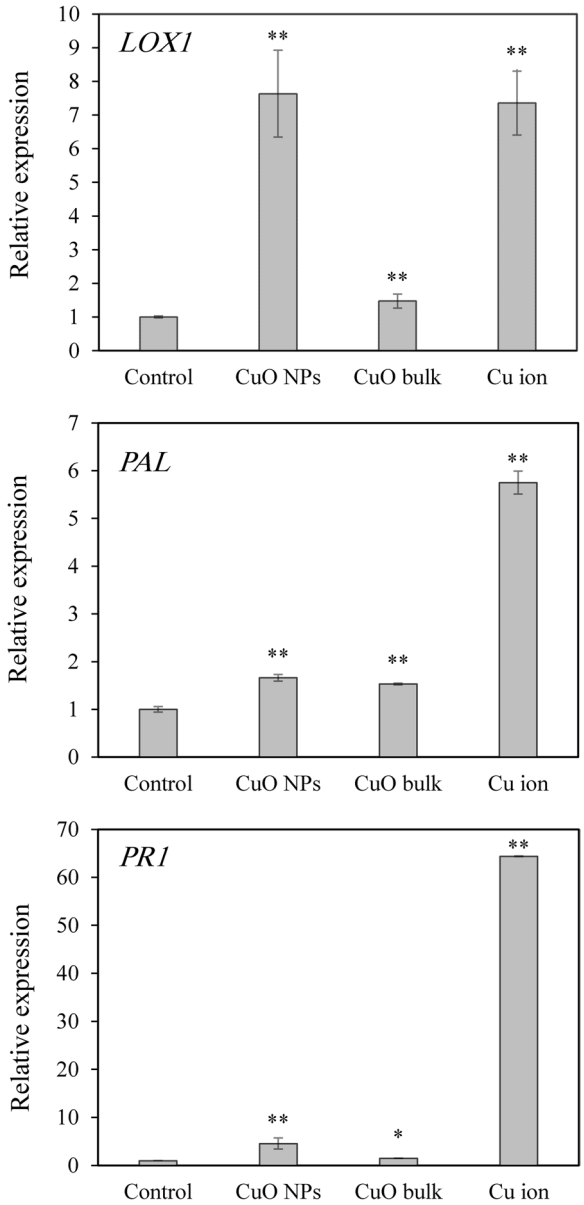

Fig. 6 Changes in expression patterns of, *LOX-1*, *PAL, and PR1* genes in barley seedlings after 3-days exposure to CuO NPs, CuO bulk, and Cu ion treatments. Values are the average of 3 independent replications ± standard error. * and**, different from control group at $P \leq 0.05$ and $P \leq 0.01$, respectively.

t-ZR and DHZ levels in barley seedlings. In line with our findings, CeO_2 NPs did not alter the t-ZR content in the leaves and roots of Bt-transgenic cotton compared to the control group [71].

The contribution of GAs to plant growth, development, and response to stressors is significant [74]. The impacts of nanoparticles on the content of endogenous gibberellin in plants have been documented [75, 76]. The results of the present study revealed that the use of CuO NPs, CuO bulk, and Cu^{2+} ion treatments led to a reduction in gibberellin (GA_1, GA_4, and GA_9) levels. Similar to our results, the concentration of GA decreased significantly upon exposure to different doses of CuO NPs (10, 200, and 1000 $mg.L^{-1}$) in cotton leaves [71]. This phenomenon may be caused by the ability of Cu to downregulate the transcription of GAs biosynthetic pathways. In a comparative analysis, it was noted that spinach plants exposed to Cu stress displayed a protective response to stress-induced damage when exposed to lower concentrations of gibberellin through increased proline and antioxidant enzyme contents. Conversely, these parameters were adversely affected by higher concentrations of gibberellin, resulting in higher oxidative damage [77].

Exposure to nanoparticles is likely to elicit a rapid response in the ABA signaling pathway of plants [78, 79]. Our results indicated that the ABA content in barley leaves significantly increased following exposure Cu NPs, CuO bulk, and Cu^{2+} ions. Our results are corroborated by the findings of Le Van et al. which observed a rise in ABA levels of cotton exposed to the high concentrations of CuO NPs (200 and 1000 $mg.L^{-1}$) [80]. Similarly, Yue et al. found that La_2O_3 nanoparticles increased the ABA content in maize seedlings, causing the ABA receptor to activate the ABA signaling pathway and improve stress tolerance by triggering the plant's antioxidant defense mechanisms [81]. Vankova et al. found that exposure to various concentrations of ZnO NPs (20 and 100 mg L^{-1}) resulted in a significant increase of ABA content in *A. thaliana's* leaves and apices [72]. The elevation in ABA content in Arabidopsis plants exposed to Ag NPs was consistent with the increased expression of *NCED3* and *RD22*, two genes related to the biosynthesis and signaling of ABA [27, 72]. The protective mechanisms of ABA against metal NPs may be similar to its role in response to metal ions stresses. Our results demonstrated a similar increase in ABA content in CuO NPs and Cu^{2+} ion treatment in barley leaves. Tao et al. discovered that the application of ABA on grapevine and lettuce plants under Cd and Zn stress resulted in a decrease in metal bioaccumulation, increased biomass, and up-regulated the zinc/iron transporter protein (ZIP) family [82]. Additionally, Song et al. also demonstrate that ABA plays a key role in the mitigation of Zn toxicity by enhancing the expression of genes that are associated with the detoxification of heavy metals in grapevine plants [83]. The occurrence of ABRE (ABA-responsive elements) in specific gene promoter regions indicates that ABA has a notable impact on gene expression when subjected to metal stress, including exposure to gold nanoparticles [84]. In a study on Cd-stressed rice, the overexpression of the Os*NCED4* gene was observed, which suggests the importance of ABA in coping with Cd toxicity [85].

The ISR pathway is induced by the accumulation of ET and JA, and plays crucial roles as a fundamental component of the plant immune system. Our study revealed that exposure to CuO NPs, Cu^{2+} ions, and CuO bulk led to a significant rise in ethylene content in barley. This finding is in line with previous studies from Azhar et al. and Khan et al. demonstrating a correlation between nanoparticle exposure and an increase in ET biosynthesis and signaling in plants [59, 86]. Moreover, Asgher et al. and Betti et al. reported that plants can reduce the negative effects of environmental stresses (including trace elements) by producing more ET, which serves as a defense mechanism to alleviate oxidative damage [87, 88]. More specifically, Rather et al. observed elevated levels of ET in the leaves of *Brassica nigra* when exposed to copper-induced oxidative stress [89]. This was likely due to the activation of *ACS* genes responsible for ET biosynthesis. Metal toxicity is presumed to amplify the expression of *ACO* and *ACS* genes coding two enzymes in ET biosynthesis in plants leading to an increase in ET production [86]. Additionally, Cu accumulation can lead to the upregulation of *ERF*-responding and *ACS* genes which can result in an overproduction of ethylene as a means to ++regulate oxidative stress [90].

Jasmonic acid (JA) is synthesized through the activity of the *LOX-1* enzyme and originates from polyunsaturated fatty acids. Its crucial role in regulating the induced systemic resistance (ISR) pathway has been well-established [91, 92]. When plants are exposed to biotic and abiotic stresses, the levels of JA, precursors, and derivatives increase. These compounds can improve the plants' chemical defense and resistance against stress [93]. For instance, Jasmonates have been found to assist plants in coping with metal-induced stress caused by Cd, As, Pb, Cu and Ni [94]. Our findings revealed that the foliar application of Cu^{2+} ions and CuO NPs have significantly increased the endogenous concentrations of JA in barley. Kasote et al. reported that JA-mediated defense responses are induced after the priming of watermelon seeds with a low concentration of Fe NPs [95]. CuO NPs treatment in *A. thaliana* also led to modification in the JA pathway by upregulation of its precursors (e.g. dinor-12-Oxo-phytodienoic acid) [96]. Furthermore, Shang et al. found that copper sulfide nanoparticles also increased the JA production in *Oryza sativa* against fungal infection by *Gibberella fujikuroi* [97]. Accumulation of JA in *A. thaliana* leaves in response to low concentrations of ZnO NPs has been reported [72].

Nanoparticles have been shown to alter salicylic acid (SA) levels in plants, which modifies resistance against viral infections, increases biomass, and activates antioxidant systems [79, 98]. In the present study, the application of CuO NPs, CuO bulk, and Cu^{2+} ions led to a significant reduction in SA content. This effect can be ascribed to the antagonism between SA and ABA [72]. It has been well documented that ABA promotes the down-regulation of SA biosynthetic components and also inhibits SA responses when the plant is under pathogen attack or stress [99, 100]. The reduction of SA levels in the present study is in line with the notable rise in ABA content due to CuO NPs, CuO bulk, and Cu^{2+} ions. Consistently, Vankova et al. reported a decrease in SA levels in apices of *A. thaliana* at high concentrations of ZnO NPs [72]. Zhao et al. indicated that the Arabidopsis plants with reduced levels of endogenous SA due to the presence of the *nahG* (naphthalene hydroxylase G) gene showed increased resistance to Cd stress [101]. In contrast, the mutant *snc1*, with higher levels of endogenous SA, was more vulnerable to Cd stress compared to the control group.

While our results confirm that Cu exposure disrupts phytohormonal homeostasis, they also highlight the differential impact of CuO NPs compared to bulk CuO. The more significant changes in IAA, GAs, ET, ABA, SA, JA, and ET in CuO NP-treated plants compared to the bulk CuO, suggest a greater capacity to induce stress response mechanisms, possibly due to their enhanced bioavailability and surface reactivity, and dissolution rate.

The ISR and SAR pathways are two forms of immune systems in plants activated by phytohormones as a result of biotic interactions [28, 29]. Nonetheless, it has been proven that abiotic stresses can also trigger the activation of these pathways. [92, 102]. SAR is triggered by SA and is associated with the transcriptional activation of PR proteins [103]. Despite the decrease in SA content in response to CuO NPs, CuO bulk and Cu^{2+} ions treatment in the present study, the expression of *PR1* significantly increased in barley seedlings. Dey et al. reported that in barley, the induction of SAR in response to pathogen attack was not associated with the endogenous SA, and alternatively, the pathway was triggered by the increase in ABA content, which is consistent with an elevated ABA content observed in the present study [104]. The induction of the ISR pathway is linked to ET and JA, causing the upregulation of various genes such as *PAL* and *LOX* [28]. In the present study, the expression of *LOX-1*, *PAL*, and *PR-1* genes was significantly increased in response to CuO NPs, CuO bulk, and Cu^{2+} ions treatment in accordance with the accumulation of phytohormones, ET, JA, and ABA. Similar findings were reported by Derbalah et al. reported that the zirconium oxide nanoparticles stimulated systemic resistance in cucumber plants infected with *Rhizoctonia solani* and caused an upregulation of *PAL1*, *PR-1*, and *LOX-1* genes [105]. Similarly, Abdelkhalek and Al-Askar. reported that spraying tomato plants with biosynthesized ZnO NPs

prior to or after inoculation with tobacco mosaic virus (TMV) increased the expression of *PAL* and *PR-1* genes [33]. In a study, Cai et al. examined the effects of Fe_3O_4 NPs through foliar spraying on *Nicotiana benthamiana* plants as a means of enhancing their defense mechanisms against TMV and reported an increased expression of PR genes [79]. Chun and Chandrasekaran. reported an increase in the expression of PR genes, specifically *PR-1* and *PR-2* (beta 1,3-glucanase), in tomato plants treated with chitosan nanoparticles after 24 hours of exposure to the wilt-inducing agent *Fusarium andiyazi* [106]. Gopalakrishnan Nair et al. observed an upsurge in *PAL* gene expression in soybean plants subjected to CuO NPs [107].

The phenylpropanoid pathway is dependent on the activity of the PAL enzyme which synthesizes a variety of phenols and flavonoids, thereby facilitating the elimination of ROS [108]. Heavy metals, including Cu, have the ability to regulate PAL and other stress-related plant enzymes [109]. Multiple studies have proven that the application of Cu and Zn could elevate the levels of *PAL* expression and activity [110–112]. Our research demonstrates a considerable upregulation of *PAL* gene expression in response to Cu^{2+}, which is consistent with Ali et al. who observed the induction of PAL activity by copper stress in root cultures of *Panax ginseng* [111]. LOX is the primary enzyme involved in the JA synthesis pathway, a crucial hormone that regulates ISR [91]. Bhardwaj et al. discovered that *LOX* expression in *Caragana jubata* plants was affected when exposed to ABA, methyl jasmonate (MJ), and SA [113]. Additionally, further stimulation of *LOX-1* expression in mature Arabidopsis plants was observed with the use of JA and nitric oxide (NO). ABA and MJ were found to have the most significant influence on *LOX-1* expression [114]. Schaffer et al. reported that in *Malus domestica*, the transcription of *LOX-1*, *LOX3*, and *LOX7* genes is induced by ethylene [115]. Moreover, it has shown that arsenic stress alters the transcription levels of *LOX* in *O. sativa* [116]. Li et al. found that JA and ABA increased the expression of *TcLOX-1* and *TcLOX-2* in *Tsuga chinensis*, but not SA, which aligns with the results of our study [117].

Based on our results, the upregulation of ISR and SAR genes in barley seedlings treated with CuO NPs, bulk CuO, and Cu^{2+} ions suggest that at high Cu concentrations, these responses are mainly due to Cu-induced stress rather than nanoparticle-specific effects. However, the higher expression of *LOX-1*, *PAL*, and *PR-1* genes in CuO NP-treated plants highlights the potential role of nanoparticles in enhancing stress signaling and response, as compared to bulk CuO, presumably by a higher rate of ROS production. These results indicate that while CuO NPs at high concentrations do not elicit unique stress responses, their physicochemical properties may exacerbate plant responses compared to bulk CuO. The distinctive properties of CuO NPs, such as their small size, high surface area, and rapid dissolution rate compared to bulk CuO, may result in a faster release of copper ions compared to bulk CuO, leading to a more acute toxicity.

Conclusions

This study demonstrated that exposure to CuO NPs, bulk CuO, and Cu^{2+} ions induced oxidative stress and activity of antioxidant enzymes, decreased nutrient concentrations, and disrupted hormonal homeostasis in barley seedlings. Our findings indicate that CuO NPs, bulk CuO, and Cu^{2+} ions led to an increase in stress-related hormonal content, including increased levels of ABA, JA, and ET leading to activations of ISR and SAR pathways by upregulation of key genes (*LOX-1, PAL, and PR-1*). While Cu^{2+} ions induced the strongest stress responses, CuO NPs elicited a more pronounced effect compared to bulk CuO, suggesting that their nanoscale properties contribute to greater physiological and molecular effects. However, the lack of a completely distinct response to CuO NPs, compared to bulk and ionic Cu, suggests that the effects of high concentrations of CuO NPs are not unique but rather an enhancement of general Cu-induced toxicity. Future research should focus on differentiating the specific nanoparticle-mediated effects rather than general Cu toxicity by controlling for ion dissolution rates or stabilized nanoparticles. A deeper mechanistic understanding of CuO NP interactions with plant cellular pathways will be essential for assessing their potential risks and benefits in agricultural applications.

Supplementary Information

The online version contains supplementary material available at https://doi.org/10.1186/s12870-025-06213-6.

Supplementary Material 1: Supplementary Table 1. The zeta potential of CuO NPs and CuO bulk

Supplementary Material 2: Supplementary Table 2. eZAF Smart Quant Results of the selected surface region in barley leaves

Supplementary Material 3: Supplementary Table 3. eZAF Smart Quant Results selected cross region of barley leaves

Supplementary Material 4: Supplementary Table 4. Primer sequences used for quantitate real-time PCR analysis

Supplementary Material 5: Supplementary Fig. 1. FESEM micrographs of CuO NPs at 200 nm (a) and 1 µm (b)

Supplementary Material 6: Supplementary Fig. 2. Particle size distribution of CuO NPs and CuO bulk using dynamic light scattering (DLS) analysis

Supplementary Material 7: Supplementary Fig. 3. XRD pattern of CuO NPs (a). Correspondence of the phases and relative intensity of the XRD spectra with the main reflection of JCPDS cards No 01–089-5895 for CuO NPs (b)

Supplementary Material 8: Supplementary Fig. 4. SEM micrographs, EDX spectra showing the presence of CuO NPs in the surface layer of barley

leaf. SEM micrographs of CuO NP treated leaf at different magnifications (a-b), Panel (c) shows EDX spectra of surface layers of barley tissue. The structure indicated by the red circle represents the agglomerated CuO NPs

Supplementary Material 9: Supplementary Fig. 5. SEM micrographs, EDX spectra showing the presence of CuO NPs in cross-layer of barley leaf. SEM micrographs of CuO NP treated leaf at different magnification (a-b), Panel (c) shows EDX spectra of cross layers of barley tissue

Acknowledgments
Not applicable

Authors' contributions
A.A.GR conceived the study and designed experiments; S.A performed experiments and analyzed the experimental data; S.A wrote the first draft of the manuscript. A.A.GR reviewed and revised the manuscript.

Funding
Not applicable

Data availability
All data generated or analysed during this study are included in this published article and its Supplementary Information files.

Declarations

Ethics approval and consent to participate
Not applicable

Consent for publication
Not applicable.

Competing interests
The authors declare no competing interests.

Received: 13 May 2024 Accepted: 6 February 2025
Published online: 13 February 2025

References

1. Du W, Yang J, Peng Q, Liang X, Mao H. Comparison study of zinc nanoparticles and zinc sulphate on wheat growth: From toxicity and zinc biofortification. Chemosphere. 2019;227:109–16. https://doi.org/10.1016/j.chemosphere.2019.03.168.
2. Klaine SJ, Alvarez PJJ, Batley GE, Fernandes TF, Handy RD, Lyon DY, et al. Nanomaterials in the environment: Behavior, fate, bioavailability, and effects. Environ Toxicol Chem. 2008;27(9):1825–51. https://doi.org/10.1897/08-090.1.
3. Reddy Pullagurala VL, Adisa IO, Rawat S, Kalagara S, Hernandez-Viezcas JA, Peralta-Videa JR, et al. ZnO nanoparticles increase photosynthetic pigments and decrease lipid peroxidation in soil grown cilantro (*Coriandrum sativum*). Plant Physiol Biochem. 2018;132:20–127. https://doi.org/10.1016/j.plaphy.2018.08.037.
4. Jeevanandam J, Barhoum A, Chan YS, Dufresne A, Danquah MK. Review on nanoparticles and nanostructured materials: History, sources, toxicity and regulation. Beilstein J Nanotechnol. 2018;3:9:1050–74. https://doi.org/10.3762/bjnano.9.98.
5. Badawy AA, Abdelfattah NAH, Salem SS, Awad MF, Fouda A. Efficacy assessment of biosynthesized copper oxide nanoparticles (CuO-NPs) on stored grain insects and their impacts on morphological and physiological traits of wheat (*triticum aestivum* l). Plant Biol. 2021;10(3):233. https://doi.org/10.3390/biology10030233.
6. Pugazhendhi A, Prabhu R, Muruganantham K, Shanmuganathan R, Natarajan S. Anticancer, antimicrobial and photocatalytic activities of green synthesized magnesium oxide nanoparticles (MgONPs) using aqueous extract of *Sargassum wightii*. J Photochem Photobiol B. 2019;190:86–97. https://doi.org/10.1016/j.jphotobiol.2018.11.014.
7. Prasad R, Bhattacharyya A, Nguyen QD. Nanotechnology in sustainable agriculture: recent developments, challenges, and perspectives. Front Microbiol. 2017;8:1014. https://doi.org/10.3389/fmicb.2017.01014.
8. Nel A, Xia T, Mädler L, Li N. Toxic potential of materials at the nanolevel. Science. 2006;3:5761. https://doi.org/10.1126/science.1114397.
9. Nair R. Plant response strategies to engineered metal oxide nanoparticles: A review. In: Phytotoxicity of Nanoparticles. Nanoscale Res Lett. 2017;12(1):92. https://doi.org/10.1186/s11671-017-1861-y.
10. Cota-Ruiz K, Delgado-Rios M, Martínez-Martínez A, Núñez-Gastelum JA, Peralta-Videa JR, Gardea-Torresdey JL. Current findings on terrestrial plants – Engineered nanomaterial interactions: Are plants capable of phytoremediating nanomaterials from soil? Curr Opin Environ Sci Health. 2018;6:9–15. https://doi.org/10.1016/j.coesh.2018.06.005.
11. Pérez-Hernández H, Fernández-Luqueño F, Huerta-Lwanga E, Mendoza-Vega J, Álvarez-Solís José D. Effect of engineered nanoparticles on soil biota: Do they improve the soil quality and crop production or jeopardize them? Land Degrad Dev. 2020;31(16):2213–30. https://doi.org/10.1002/ldr.3595.
12. Rezvani E, Rafferty A, McGuinness C, Kennedy J. Adverse effects of nanosilver on human health and the environment. Acta Biomater. 2019;94:145–59. https://doi.org/10.1016/j.actbio.2019.05.042.
13. Yan A, Chen Z. Impacts of silver nanoparticles on plants: A focus on the phytotoxicity and underlying mechanism. Int J Mol Sci. 2019;26;20(5):1003. https://doi.org/10.3390/ijms20051003
14. Reckova S, Tuma J, Dobrev P, Vankova R. Influence of copper on hormone content and selected morphological, physiological and biochemical parameters of hydroponically grown *Zea mays* plants. Plant Growth Regul. 2019;89:191–201. https://doi.org/10.1007/s10725-019-00527-w.
15. Rehman M, Liu L, Wang Q, Saleem MH, Bashir S, Ullah S, et al. Copper environmental toxicology, recent advances, and future outlook: a review. Environ Sci Pollut Res Int. 2019;26:18003–16. https://doi.org/10.1007/s11356-019-05073-6.
16. Mir AR, Pichtel J, Hayat S. Copper: uptake, toxicity and tolerance in plants and management of Cu-contaminated soil. Biometals. 2021;34:737–59. https://doi.org/10.1007/s10534-021-00306-z.
17. Alizadeh SR, Ebrahimzadeh MA. Characterization and Anticancer Activities of Green Synthesized CuO Nanoparticles, A Review. Anticancer Agents Med Chem. 2020;21(12):1529–43. https://doi.org/10.2174/1871520620666201029111532.
18. Małecki JJ, Kadzikiewicz-Schoeneich M, Szostakiewicz-Hołownia M. Concentration and mobility of copper and zinc in the hypergenic zone of a highly urbanized area. Environ Earth Sci. 2016;376(6593):603–8. https://doi.org/10.1007/s12665-015-4789-5.
19. Xiong T, Zhang S, Kang Z, Zhang T, Li S. Dose-dependent physiological and transcriptomic responses of lettuce (*Lactuca sativa* l.) to copper oxide nanoparticles—insights into the phytotoxicity mechanisms. Int J Mol Sci. 2021;22(7):3688. https://doi.org/10.3390/ijms22073688.
20. Shah IH, Manzoor MA, Sabir IA, Ashraf M, Liaquat F, Gulzar S, et al. Phytotoxic effects of chemically synthesized copper oxide nanoparticles induce physiological, biochemical, and ultrastructural changes in *Cucumis melo*. Environ Sci Pollut Res Int. 2023;30(18):51595–606. https://doi.org/10.1007/s11356-023-26039-9.
21. Wang Z, Xu L, Zhao J, Wang X, White JC, Xing B. CuO nanoparticle interaction with *Arabidopsis thaliana*: toxicity, parent-progeny transfer, and gene expression. Environ Sci Technol. 2016;50(11):6008–16. https://doi.org/10.1021/acs.est.6b01017.
22. Wang W, Ren Y, He J, Zhang L, Wang X, Cui Z. Impact of copper oxide nanoparticles on the germination, seedling growth, and physiological responses in *Brassica pekinensis* L. Environ Sci Pollut Res Int. 2020;27:31505–15. https://doi.org/10.1007/s11356-020-09338-3.
23. Rhaman MS, Imran S, Rauf F, Khatun M, Baskin CC, Murata Y, et al. Seed priming with phytohormones: An effective approach for the mitigation of abiotic stress. Plants. 2021;10(1):37. https://doi.org/10.3390/plants10010037.
24. Le Van N, Rui Y, Cao W, Shang J, Liu S, Quang TN, et al. Toxicity and bioeffects of CuO nanoparticles on transgenic Ipt-cotton. J Plant Interact. 2016;11(1):108–16. https://doi.org/10.1080/17429145.2016.1217434.

25. Gui X, Deng Y, Rui Y, Gao B, Luo W, Chen S, et al. Response difference of transgenic and conventional rice (*Oryza sativa*) to nanoparticles (γFe_2O_3). Environ Sci Pollut Res Int. 2015;22:17716–23. https://doi.org/10.1007/s11356-015-4976-7.
26. Kaveh R, Li YS, Ranjbar S, Tehrani R, Brueck CL, Van Aken B. Changes in *Arabidopsis thaliana* gene expression in response to silver nanoparticles and silver ions. Environ Sci Technol. 2013;18:10637–44. https://doi.org/10.1021/es402209w.
27. Syu Yyu, Hung JH, Chen JC, Chuang H. wen. Impacts of size and shape of silver nanoparticles on *Arabidopsis* plant growth and gene expression. Plant Physiol Biochem. 2014;83:57–64. https://doi.org/10.1016/j.plaphy.2014.07.010
28. Messa VR. Biocontrol by induced systemic resistance using plant growth promoting rhizobacteria. Rhizosphere. 2021;4:234. https://doi.org/10.3390/insects11040234.
29. 29, Romera FJ, García MJ, Lucena C, Martínez-Medina A, Aparicio MA, Ramos J, et al. Induced systemic resistance (ISR) and Fe deficiency responses in dicot plants. Front Plant Sci. 2019;10:287. https://doi.org/10.3389/fpls.2019.00287.
30. Sinha RK, Verma SS, Rastogi A. Role of pathogen-related protein 10 (PR 10) under abiotic and biotic stresses in plants. Phyton. 2020;89(2):167–82. https://doi.org/10.32604/phyton.2020;09359.
31. Jiang L, Wu J, Fan S, Li W, Dong L, Cheng Q, et al. Isolation and characterization of a novel pathogenesis-related protein gene (GmPRP) with induced expression in soybean (*Glycine max*) during infection with *Phytophthora sojae*. PLoS ONE. 2015;10(6):e0129932. https://doi.org/10.1371/journal.pone.0129932.
32. Seo PJ, Lee AK, Xiang F, Park CM. Molecular and functional profiling of *Arabidopsis pathogenesis*-related genes: Insights into their roles in salt response of seed germination. Plant Cell Physiol. 2008;3:334–44. https://doi.org/10.1093/pcp/pcn011.
33. Abdelkhalek A, Al-Askar AA. Green synthesized ZnO nanoparticles mediated by *Mentha spicata* extract induce plant systemic resistance against Tobacco mosaic virus. Appl Sci. 2020;10(15):5054. https://doi.org/10.3390/app10155054.
34. Ngigi AN, Muraguri BM. ICP-OES determination of essential and non-essential elements in *Moringa oleifera*, *Salvia hispanica* and *Linum usitatissimum*. Sci Afr. 2019;6:e00165. https://ui.adsabs.harvard.edu/link_gateway/2019SciAf… N/doi:10.1016/j.sciaf.2019.e00165.
35. Alexieva V, Sergiev I, Mapelli S, Karanov E. The effect of drought and ultraviolet radiation on growth and stress markers in pea and wheat. Plant Cell Environ. 2001;12:1337–44. https://doi.org/10.1046/j.1365-3040.2001.00778.x.
36. Bradford MM. A rapid and sensitive method for the quantitation of microgram quantities of protein utilizing the principle of protein-dye binding. Anal Biochem. 1976;72:248–54. https://doi.org/10.1016/0003-2697(76)90527-3.
37. Aebi H. Catalase in in vitro. Methods Enzymol. 1984;105:121–6. https://doi.org/10.1016/s0076-6879(84)05016-3.
38. Nakano Y, Asada K. Purification of ascorbate peroxidase in spinach chloroplasts; its inactivation in ascorbate-depleted medium and reactivation by monodehydroascorbate radical. Plant Cell Physiol. 1987;28:131–40. https://doi.org/10.1093/oxfordjournals.pcp.a077268.
39. Giannopolitis CN, Ries SK. Superoxide dismutases: I. Occurrence in higher plants. Plant Physiol. 1977;59(2):309–. https://doi.org/10.1104/pp.59.2.309. 14.
40. Singh DP, Prabha R, Yandigeri MS, Arora DK. Cyanobacteria-mediated phenylpropanoids and phytohormones in rice (*Oryza sativa*) enhance plant growth and stress tolerance. Antonie Van Leeuwenhoek. 2011;100(4):557–68. https://doi.org/10.1007/s10482-011-9611-0.
41. Liu S, Chen W, Qu L, Gai Y, Jiang X. Simultaneous determination of 24 or more acidic and alkaline phytohormones in femtomole quantities of plant tissues by high-performance liquid chromatography-electrospray ionization-ion trap mass spectrometry. Anal Bioanal Chem. 2013;405(4):1257–66. https://doi.org/10.1007/s00216-012-6509-2.
42. Ahangir A, Ghotbi-Ravandi AA, Rezadoost H, Bernard F. Drought tolerant maize cultivar accumulates putrescine in roots. Rhizosphere. 2020;16:100260. https://doi.org/10.1016/j.rhisph.2020.100260.
43. Pfaffl MW, Horgan GW, Dempfle L. Relative expression software tool (REST©) for group-wise comparison and statistical analysis of relative expression results in real-time PCR. Nucleic Acids Res. 2002;30:e36–36. https://doi.org/10.1093/nar/30.9.e36.
44. Rizwan M, Ali S, Qayyum MF, Ok YS, Adrees M, Ibrahim M, et al. Effect of metal and metal oxide nanoparticles on growth and physiology of globally important food crops: A critical review. J Hazard Mater. 2017;322:2–16. https://doi.org/10.1016/j.jhazmat.2016.05.061.
45. Mahmoodzadeh H, Aghili R, Nabavi M. Physiological effects of TiO_2 nanoparticles on wheat (*Triticum aestivum*). Tech J Eng Appl Sci. 2013;3:1365–70.
46. Nair PMG, Chung IM. A mechanistic study on the toxic effect of copper oxide nanoparticles in soybean (*Glycine max* L.) root development and lignification of root cells. Biol Trace Elem Res. 2014;162:342–52. https://doi.org/10.1007/s12011-014-0106-5.
47. Zaheer IE, Ali S, Rizwan M, Farid M, Shakoor MB, Gill RA, et al. Citric acid assisted phytoremediation of copper by *Brassica napus* L. Ecotoxicol Environ Saf. 2015;120:307–10. https://doi.org/10.1016/j.ecoenv.2015.06.020.
48. Rizwan M, Ali S, Adrees M, Rizvi H, Zia-ur-Rehman M, Hannan F, et al. Cadmium stress in rice: toxic effects, tolerance mechanisms, and management: a critical review. Environ Sci Pollut Res. 2016;23(18):17859–79. https://doi.org/10.1007/s11356-016-6436-4.
49. Rizwan M, Ali S, Abbas T, Zia-ur-Rehman M, Hannan F, Keller C, et al. Cadmium minimization in wheat: A critical review. Ecotoxicol Environ Saf. 2016;130:43–53. https://doi.org/10.1016/j.ecoenv.2016.04.001.
50. Shams G, Ranjbar M, Amiri AA, Khodarahmpour Z. The effect of 35 nm silver nanoparticles on antagonistic and synergistic mineral elements in leaves and fruit of tomato (*Lycopersicon esculentum* Mill). Int J Agricul Crop Sci. 2013;5:493–500.
51. Dimkpa CO, McLean JE, Britt DW, Anderson AJ. Nano-CuO and interaction with nano-ZnO or soil bacterium provide evidence for the interference of nanoparticles in metal nutrition of plants. Ecotoxicol. 2015;24:119–29. https://doi.org/10.1007/s10646-014-1364-x.
52. Peralta-Videa JR, Hernandez-Viezcas JA, Zhao L, Diaz BC, Ge Y, Priester JH, et al. Cerium dioxide and zinc oxide nanoparticles alter the nutritional value of soil cultivated soybean plants. Plant Physiol Biochem. 2014;80:128–35. https://doi.org/10.1016/j.plaphy.2014.03.028.
53. Le VN, Rui Y, Gui X, Li X, Liu S, Han Y. Uptake, transport, distribution and bio-effects of SiO_2 nanoparticles in Bt-transgenic cotton. J Nanobiotechnol. 2014;12:1–15. https://doi.org/10.1186/s12951-014-0050-8.
54. Li X, Gui X, Rui Y, Ji W, Yu Z, Peng S. Bt-transgenic cotton is more sensitive to CeO_2 nanoparticles than its parental non-transgenic cotton. J Hazard Mater. 2014;274:173–80. https://doi.org/10.1016/j.jhazmat.2014.04.025.
55. Corral-Diaz B, Peralta-Videa JR, Alvarez-Parrilla E, Rodrigo-García J, Morales MI, Osuna-Avila P, et al. Cerium oxide nanoparticles alter the antioxidant capacity but do not impact tuber ionome in *Raphanus sativus* (L). Plant Physiol Biochem. 2014;84:277–85. https://doi.org/10.1016/j.plaphy.2014.09.018.
56. Hong J, Rico CM, Zhao L, Adeleye AS, Keller AA, Peralta-Videa JR, et al. Toxic effects of copper-based nanoparticles or compounds to lettuce (*Lactuca sativa*) and alfalfa (*Medicago sativa*). Environ Sci Processe Impacts. 2015;17(1):177–85. https://doi.org/10.1039/c4em00551a.
57. Ojha NK, Zyryanov GV, Majee A, Charushin VN, Chupakhin ON, Santra S. Copper nanoparticles as inexpensive and efficient catalyst: A valuable contribution in organic synthesis. Coord Chem Rev. 2017;353:1–57. https://doi.org/10.1016/j.ccr.2017.10.004.
58. Rather BA, Masood A, Sehar Z, Majid A, Anjum NA, Khan NA. Mechanisms and role of nitric oxide in phytotoxicity-mitigation of copper. Front Plant Sci. 2020;11:675. https://doi.org/10.3389/fpls.2020.00675.
59. Azhar W, Khan AR, Muhammad N, Liu B, Song G, Hussain A, et al. Ethylene mediates CuO NP-induced ultrastructural changes and oxidative stress in: *Arabidopsis thaliana* leaves. Environ Sci Nano. 2020;7:938–53. https://doi.org/10.1039/C9EN01302D.
60. Chung I-M, Rekha K, Venkidasamy B, Thiruvengadam M. Effect of copper oxide nanoparticles on the physiology, bioactive molecules, and transcriptional changes in *Brassica rapa* ssp. rapa seedlings. Water Air Soil Pollut. 2019;230:1–14. https://doi.org/10.1007/s11270-019-4084-2.
61. Rather BA, Mir IR, Masood A, Anjum NA, Khan NA. Nitric oxide pretreatment advances seed germination and alleviates copper-induced photosynthetic inhibition in Indian mustard. Plants. 2020;9:776. https://doi.org/10.3390/plants9060776.

62. Mir IR, Rather BA, Masood A, Majid A, Sehar Z, Anjum NA, et al. Soil sulfur sources differentially enhance cadmium tolerance in Indian mustard (*Brassica juncea* L). Soil Syst. 2021;5:29. https://doi.org/10.3390/soilsystems5020029.
63. Anjum NA, Sharma P, Gill SS, Hasanuzzaman M, Khan EA, Kachhap K, et al. Catalase and ascorbate peroxidase—representative H_2O_2-detoxifying heme enzymes in plants. Environ Sci pollut Res Int. 2016;23:19002–29. https://doi.org/10.1007/s11356-016-7309-6.
64. Faizan M, Faraz A, Yusuf M, Khan ST, Hayat S. Zinc oxide nanoparticle-mediated changes in photosynthetic efficiency and antioxidant system of tomato plants. Photosynthetica. 2018;56:678–86. https://doi.org/10.1007/s11099-017-0717-0.
65. Yusefi-Tanha E, Fallah S, Rostamnejadi A, Pokhrel LR. Particle size and concentration dependent toxicity of copper oxide nanoparticles (CuONPs) on seed yield and antioxidant defense system in soil grown soybean (*Glycine max* cv. Kowsar). Sci Total Environ. 2020;715:136994. https://doi.org/10.1016/j.scitotenv.2020.136994.
66. Tamez C, Hernandez-Molina M, Hernandez-Viezcas JA, Gardea-Torresdey JL. Uptake, transport, and effects of nano-copper exposure in zucchini (*Cucurbita pepo*). Sci Total Environ. 2019;665:100–6. https://doi.org/10.1016/j.scitotenv.2019.02.029.
67. Pooja P, Nandwal AS, Chand M, Pal A, Kumari A, Rani B, et al. Soil moisture deficit induced changes in antioxidative defense mechanism of sugarcane (*Saccharum officinarum*) varieties differing in maturity. Indian J Agri Sci. 2020;90(3). https://doi.org/10.56093/ijas.v90i3.101458. 507 – 12.
68. Rather BA, Mir IR, Sehar Z, Anjum NA, Masood A, Khan NA. The outcomes of the functional interplay of nitric oxide and hydrogen sulfide in metal stress tolerance in plants. Plant Physiol Biochem. 2020;155:523–34. https://doi.org/10.1016/j.plaphy.2020.08.005.
69. Sytar O, Kumari P, Yadav S, Brestic M, Rastogi A. Phytohormone priming: regulator for heavy metal stress in plants. J Plant Growth Regul. 2019;38:739–52. https://doi.org/10.1007/s00344-018-9886-8.
70. Rasool N. Plant Hormones: Role in Alleviating Biotic Stress. In: Plant Hormones - Recent Advances, New Perspectives and Applications (ed Hano C). 2022. https://doi.org/10.5772/intechopen.102689
71. Singh Brar R, Kumar A, Kaur S, Saha S, Kumar A, Kumar S. Impact of metal oxide nanoparticles on cotton (*Gossypium hirsutum* L.): a physiological perspective. J Cotton Res. 2021. https://doi.org/10.1186/s42397-021-00092-6. 4;16.
72. Vankova R, Landa P, Podlipna R, Dobrev PI, Prerostova S, Langhansova L, et al. ZnO nanoparticle effects on hormonal pools in *Arabidopsis thaliana*. Sci Total Environ. 2017;593–594:535–42. https://doi.org/10.1016/j.scitotenv.2017.03.160.
73. Sun J, Wang L, Li S, Yin L, Huang J, Chen C. Toxicity of silver nanoparticles to Arabidopsis: Inhibition of root gravitropism by interfering with auxin pathway. Environ Toxicol Chem. 2017;36(10):2773–80. https://doi.org/10.1002/etc.3833.
74. Jamla M, Khare T, Joshi S, Patil S, Penna S, Kumar V. Omics approaches for understanding heavy metal responses and tolerance in plants. Curr Plant Biol. 2021. https://doi.org/10.1016/j.cpb.2021.100213. 27;10213.
75. Hao Y, Yu F, Lv R, Ma C, Zhang Z, Rui Y, et al. Carbon nanotubes filled with different ferromagnetic alloys affect the growth and development of rice seedlings by changing the C: N ratio and plant hormones concentrations. PLoS ONE. 2016;11:e0157264. https://doi.org/10.1371/journal.pone.0157264.
76. Sheteiwy MS, Dong Q, An J, Song W, Guan Y, He F, et al. Regulation of ZnO nanoparticles-induced physiological and molecular changes by seed priming with humic acid in *Oryza sativa* seedlings. Plant Growth Regul. 2017;83:27–41. https://doi.org/10.1007/s10725-017-0281-4.
77. Gong Q, Li Zhua, Wang L, Zhou J, yi, Kang Q, Niu D. dan. Gibberellic acid application on biomass, oxidative stress response, and photosynthesis in spinach (*Spinacia oleracea* L.) seedlings under copper stress. Environ Sci Pollut Res Int. 2021;28(38):53594–53604. https://doi.org/10.1007/s11356-021-13745-5
78. Zahedi SM, Abdelrahman M, Hosseini MS, Hoveizeh NF, Tran LSP. Alleviation of the effect of salinity on growth and yield of strawberry by foliar spray of selenium-nanoparticles. Environ Pollut. 2019;253:246–58. https://doi.org/10.1016/j.envpol.2019.04.078.
79. Cai L, Cai L, Jia H, Liu C, Wang D, Sun X. Foliar exposure of Fe_3O_4 nanoparticles on *Nicotiana benthamiana*: Evidence for nanoparticles uptake, plant growth promoter and defense response elicitor against plant virus. J Hazard Mater. 2020;393:122415. https://doi.org/10.1016/j.jhazmat.2020.122415.
80. Le Van N, Ma C, Shang J, Rui Y, Liu S, Xing B. Effects of CuO nanoparticles on insecticidal activity and phytotoxicity in conventional and transgenic cotton. Chemosphere. 2016;144:661–70. https://doi.org/10.1016/j.chemosphere.2015.09.028.
81. Yue L, Chen F, Yu K, Xiao Z, Yu X, Wang Z, et al. Early development of apoplastic barriers and molecular mechanisms in juvenile maize roots in response to La_2O_3 nanoparticles. Sci Total Environ. 2019;653:675–83. https://doi.org/10.1016/j.scitotenv.2018.10.320.
82. Tao Q, Jupa R, Dong Q, Yang X, Liu Y, Li B, et al. Abscisic acid-mediated modifications in water transport continuum are involved in cadmium hyperaccumulation in *Sedum alfredii*. Chemosphere. 2021;268:129339. https://doi.org/10.1016/j.chemosphere.2020.129339.
83. Song C, Yan Y, Rosado A, Zhang Z, Castellarin SD. ABA alleviates uptake and accumulation of zinc in grapevine (*Vitis vinifera* L.) by inducing expression of ZIP and detoxification-related genes. Front Plant Sci. 2019;10:872. https://doi.org/10.3389/fpls.2019.00872.
84. Shukla D, Krishnamurthy S, Sahi SV. Genome wide transcriptome analysis reveals ABA mediated response in arabidopsis during gold ($AuCl^-_4$) treatment. Front Plant Sci. 2014;5:652. https://doi.org/10.3389/fpls.2014.00652.
85. Tan Y, Li M, Yang Y, Sun X, Wang N, Liang B et al. Overexpression of *MpCYS4*, a phytocystatin gene from *Malus prunifolia* (Willd.) Borkh., enhances stomatal closure to confer drought tolerance in transgenic arabidopsis and apple. Front Plant Sci. 2017;8:33. https://doi.org/10.3389/fpls.2017.00033
86. Khan AR, Wakeel A, Muhammad N, Liu B, Wu M, Liu Y, et al. Involvement of ethylene signaling in zinc oxide nanoparticle-mediated biochemical changes in *Arabidopsis thaliana* leaves. Environ Sci Nano. 2019;6:341–55. https://doi.org/10.1039/C8EN00971F.
87. Asgher M, Khan MIR, Anjum NA, Verma S, Vyas D, Per TS, et al. Ethylene and polyamines in counteracting heavy metal phytotoxicity: A crosstalk perspective. J Plant Growth Regul. 2018;37:1050–65. https://doi.org/10.1007/s00344-018-9823-x.
88. Betti C, Della Rovere F, Piacentini D, Fattorini L, Falasca G, Altamura MM. Jasmonates, ethylene and brassinosteroids control adventitious and lateral rooting as stress avoidance responses to heavy metals and metalloids. Biomolecules. 2021;11(1):77. https://doi.org/10.3390/biom11010077.
89. Rather BA, Mir IR, Masood A, Anjum NA, Khan NA. Ethylene-nitrogen synergism induces tolerance to copper stress by modulating antioxidant system and nitrogen metabolism and improves photosynthetic capacity in mustard. Environ Sci Pollut Res. 2022;29(32):49029–49. https://doi.org/10.1007/s11356-022-19380-y.
90. Weber LM, He J, Bradley B, Haskins K, Anseth KS. PEG-based hydrogels as an in vitro encapsulation platform for testing controlled β-cell microenvironments. Acta Biomater. 2006;2(1):1–8. https://doi.org/10.1016/j.actbio.2005.10.005.
91. Kamel SM, Elgobashy SF, Omara RI, Derbalah AS, Abdelfatah M, El-Shaer A, et al. Antifungal activity of copper oxide nanoparticles against root rot disease in cucumber. J Fungi. 2022;8:911. https://doi.org/10.3390/jof8090911.
92. Ali MS, Baek KH. Jasmonic acid signaling pathway in response to abiotic stresses in plants. Int J Mol Sci. 2020;21(2):621. https://doi.org/10.3390/ijms21020621.
93. Cohen S, Flescher E. Methyl jasmonate: A plant stress hormone as an anti-cancer drug. Phytochemistry. 2009;70(13–14):1600–9. https://doi.org/10.1016/j.phytochem.2009.06.007.
94. Dai Z, Yuan Y, Huang H, Hossain MM, Xiong S, Cao M, et al. Methyl jasmonate mitigates high selenium damage of rice via altering antioxidant capacity, selenium transportation and gene expression. Sci Total Environ. 2021;756:143848. https://doi.org/10.1016/j.scitotenv.2020.143848.
95. Kasote DM, Lee JHJ, Jayaprakasha GK, Patil BS. Seed Priming with iron oxide nanoparticles modulate antioxidant potential and defense-linked hormones in watermelon seedlings. ACS Sustain Chem Eng. 2019;7(5):5142–51. https://doi.org/10.1021/acssuschemeng.8b06013.
96. Chavez Soria NG, Bisson MA, Atilla-Gokcumen GE, Aga DS. High-resolution mass spectrometry-based metabolomics reveal the disruption of

jasmonic pathway in *Arabidopsis thaliana* upon copper oxide nanoparticle exposure. Sci Total Environ. 2019;693:133443. https://doi.org/10.1016/j.scitotenv.2019.07.249.
97. Shang H, Ma C, Li C, White JC, Polubesova T, Chefetz B, et al. Copper sulfide nanoparticles suppress *Gibberella fujikuroi* infection in rice (*Oryza sativa* L.) by multiple mechanisms: contact-mortality, nutritional modulation and phytohormone regulation. Environ Sci Nano. 2020;7:2632–43. https://doi.org/10.1039/D0EN00535E.
98. El-Shetehy M, Moradi A, Maceroni M, Reinhardt D, Petri-Fink A, Rothen-Rutishauser B, et al. Silica nanoparticles enhance disease resistance in Arabidopsis plants. Nat Nanotechnol. 2021;16:344–53. https://doi.org/10.1038/s41565-020-00812-0.
99. de Torres Zabala M, Bennett MH, Truman WH, Grant MR. Antagonism between salicylic and abscisic acid reflects early host–pathogen conflict and moulds plant defence responses. Plant J. 2009;59(3):375–86. https://doi.org/10.1111/j.1365-313X.2009.03875.x.
100. La VH, Lee BR, Islam MT, Park SH, Lee H, Bae DW, et al. Antagonistic shifting from abscisic acid- to salicylic acid-mediated sucrose accumulation contributes to drought tolerance in *Brassica napus*. Environ Exp Bot. 2019;162:38–47. https://doi.org/10.1016/j.envexpbot.2019.02.001.
101. Zhao Q, Gu C, Sun Y, Li G, Li LL, Hao L. Root defense in salicylic acid-altering Arabidopsis plants in responses to cadmium stress. J Plant Growth Regul. 2021;40:1764–76. https://doi.org/10.1007/s00344-020-10233-x.
102. Neyshabouri FA, Ghotbi-Ravandi AA, Shariatmadari Z, Tohidfar M. Cadmium toxicity promotes hormonal imbalance and induces the expression of genes involved in systemic resistances in barley. Biometals. 2024;37:1147–60. https://doi.org/10.1007/s10534-024-00597-y.
103. Shine MB, Xiao X, Kachroo P, Kachroo A. Signaling mechanisms underlying systemic acquired resistance to microbial pathogens. Plant Sci. 2019;279:81–6. https://doi.org/10.1016/j.plantsci.2018.01.001.
104. Dey S, Wenig M, Langen G, Sharma S, Kugler KG, Knappe C, et al. Bacteria-triggered systemic immunity in barley is associated with WRKY and ETHYLENE RESPONSIVE FACTORs but not with salicylic acid. Plant Physiol. 2014;166(4):2133–51. https://doi.org/10.1104/pp.114.249276.
105. Derbalah A, Elsharkawy MM, Hamza A, El-Shaer A. Resistance induction in cucumber and direct antifungal activity of zirconium oxide nanoparticles against *Rhizoctonia solani*. Pestic Biochem Physiol. 2019;157:230–6. https://doi.org/10.1016/j.pestbp.2019.03.018.
106. Chun S-C, Chandrasekaran M. Chitosan and chitosan nanoparticles induced expression of pathogenesis-related proteins genes enhances biotic stress tolerance in tomato. Int J Biol Macromol. 2019;125:948–54. https://doi.org/10.1016/j.ijbiomac.2018.12.167.
107. Gopalakrishnan Nair PM, Kim SH, Chung IM. Copper oxide nanoparticle toxicity in mung bean (*Vigna radiata* L.) seedlings: physiological and molecular level responses of in vitro grown plants. Acta Physiol Plant. 2014;36:2947–58. https://doi.org/10.1007/s11738-014-1667-9.
108. Wang C, Lu J, Zhang S, Wang P, Hou J, Qian J. Effects of Pb stress on nutrient uptake and secondary metabolism in submerged macrophyte *Vallisneria natans*. Ecotoxicol Environ Saf. 2011;74:1297–303. https://doi.org/10.1016/j.ecoenv.2011.03.005.
109. Mishra B, Singh Sangwan N. Amelioration of cadmium stress in *Withania somnifera* by ROS management: active participation of primary and secondary metabolism. Plant Growth Regul. 2019;87:403–12. https://doi.org/10.1007/s10725-019-00480-8.
110. Castañeda P, Pérez LM. Calcium ions promote the response of Citrus limon against fungal elicitors or wounding. Phytochemistry. 1996;42:595–8. https://doi.org/10.1016/0031-9422(95)00981-7.
111. Ali MB, Singh N, Shohael AM, Hahn EJ, Paek K-Y. Phenolics metabolism and lignin synthesis in root suspension cultures of *Panax ginseng* in response to copper stress. Plant Sci. 2006;171:147–54. https://doi.org/10.1016/j.plantsci.2006.03.005.
112. Van De Mortel JE, Almar Villanueva L, Schat H, Kwekkeboom J, Coughlan S, Moerland PD, et al. Large expression differences in genes for iron and zinc homeostasis, stress response, and lignin biosynthesis distinguish roots of *Arabidopsis thaliana* and the related metal hyperaccumulator *Thlaspi caerulescens*. Plant Physiol. 2006;142:1127–47. https://doi.org/10.1104/pp.106.082073.
113. Bhardwaj PK, Kaur J, Sobti RC, Ahuja PS, Kumar S. Lipoxygenase in *Caragana jubata* responds to low temperature, abscisic acid, methyl jasmonate and salicylic acid. Gene. 2011;483:49–53. https://doi.org/10.1016/j.gene.2011.05.014.
114. Viswanath KK, Varakumar P, Pamuru RR, Basha SJ, Mehta S, Rao AD. Plant Lipoxygenases and Their Role in Plant Physiology. J Plant Biol. 2020;63:83–95. https://doi.org/10.1007/s12374-020-09241-x.
115. Schaffer RJ, Friel EN, Souleyre EJF, Bolitho K, Thodey K, Ledger S, et al. A genomics approach reveals that aroma production in apple is controlled by ethylene predominantly at the final step in each biosynthetic pathway. Plant Physiol. 2007;144(4):1899–912. https://doi.org/10.1104/pp.106.093765.
116. Di X, Zheng F, Norton GJ, Beesley L, Zhang Z, Lin H, et al. Physiological responses and transcriptome analyses of upland rice following exposure to arsenite and arsenate. Environ Exp Bot. 2021;183:104366. https://doi.org/10.1016/j.envexpbot.2020.104366.
117. Li Stao, Zhang M, Fu C, hua, Xie S, Zhang Y, Yu L. jiang. Molecular Cloning and Characterization of Two 9-Lipoxygenase Genes from *Taxus chinensis*. Plant Mol Biol Report. 2012;30:1283–1290. https://doi.org/10.1007/s11105-012-0439-1

Publisher's Note